The Role of Solvent Friction in an Orbital Symmetry Controlled Reaction: Ring Closure of a Carbonyl Ylide to *cis*-2,3-Diphenyloxirane

Matthew Lipson and Kevin S. Peters*

Department of Chemistry and Biochemistry, University of Colorado, Boulder, Colorado 80309-0215

Received: November 13, 1997; In Final Form: January 9, 1998

The dynamics of the orbital symmetry controlled ring closure of the *trans*-ylide, formed upon the 266 nm photolysis of *trans*-2,3-diphenyloxirane, to produce *cis*-2,3-diphenyloxirane is examined in a variety of *n*-alkane solvents as a function of temperature. An unsuccessful attempt was made to model the kinetics within the theoretical framework developed by Kramers for a one-dimensional reaction coordinate. A model developed by Grote and Hynes that employs a frequency-dependent friction was found to give a significantly better fit to the experimental data. The possibility that a multidimensional reaction coordinate is necessary to describe the reaction dynamics is discussed.

Introduction

The role that orbital symmetry has in controlling the stereochemical outcome of organic reactions continues to be an extensively explored subject, from both theoretical and experimental perspectives. High-level theoretical calculations have revealed the nature of transition states for a wide array of pericyclic reactions that include sigmatropic shifts, electrocyclizations, cycloadditions, and cheletropic reactions.[1] The effect that solvent has on reaction paths has been explored through Monte Carlo simulations.[2,3] The nature of dynamics for the reaction system passing through the transition state is now being pursued,[4] and the suggestion that the stereoselectivity may be dynamic in origin and not controlled by the conservation of orbital symmetry has recently been presented.[5,6] Finally, the real time dynamics for passage through the transition state for a pericyclic reaction has now been achieved.[7]

Our interest in pericyclic reactions stems from our studies of the effect that solvent has in controlling the dynamics of a wide variety of organic reactions. We have recently shown that, in alkane solvents, the thermal ring closure of the carbonyl ylide (*trans*-ylide, Scheme 1) formed in 400 ps by ultraviolet photolysis of *trans*-diphenyloxirane (TDPO) decays solely via an orbital symmetry predicted pathway to form exclusively *cis*-diphenyloxirane (CDPO).[8] The decay of the *trans*-ylide involves a conrotatory processes occurring on the 600 ns time scale at room temperature.

One question that arises regarding the nature of the conrotatory process is how the dimensionality of the transition state should be view as the system passes through the transition state. Associated with the transition state is one vibrational coordinate whose frequency is imaginary.[5] Since there is one vibrational coordinate that leads to passage through the transition state, should the reaction coordinate then be viewed as effectively one-dimensional or with the additional consideration of solvent does passage through the transition state become inherently multidimensional?

For the past 15 years there has been an enormous effort undertaken in trying to understand the effect that solvent has upon dynamics of reactions that are viewed as being one-dimensional.[9] The reaction kinetics have been analyzed within the theoretical framework developed for a one-dimensional reaction coordinate by Kramers which relates the rate of a chemical reaction to the frictional coupling between solute and solvent.[10] Qualitatively, at low pressure and hence low friction, the dynamics of energy transfer from the solvent to the solute is rate limiting, and the reaction rate increases with pressure.[9,11] At the high pressure−high friction limit, passage along the molecule's reaction coordinate becomes rate limiting, and thus an increase in friction decreases the rate of the reaction. In an intermediate region of friction, the Kramers turnover region, small changes in friction have little effect on the rate of the chemical reaction.[11]

SCHEME 1

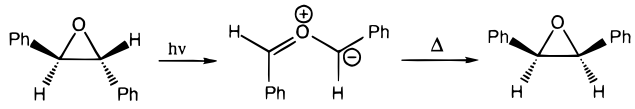

The one great difficulty in the analysis of reaction dynamics within the Kramer model has been in establishing a measure of the solvent friction felt by the solute. For the excited-state isomerization of *trans*-stilbene and related polyenes, the initial attempts to relate the solvent friction to the solvent's shear viscosity led to a failure of the Kramers model in describing the observed solvent dependence of the rate constant.[12−15] Microviscosities for a homologous solvent series, derived from rotational reorientation times for *trans*-stilbene, were found to give significantly improved fits of the Kramers model to observed reaction rates.[15−17] Finally, an excellent fit of the Kramers model to stilbene's dynamics in alkane solvents was achieved when the microfriction coefficients were derived from the translational diffusion coefficients for toluene in the *n*-alkanes.[18−20]

Troe and co-workers have suggested, on the basis of pressure and temperature studies of stilbene isomerization, that the intrinsic barrier for isomerization is solvent dependent for the *n*-alkane homologous solvent series and that it is the sensitivity of the intrinsic barrier to solvent that precludes the global fit of the kinetic data in the *n*-alkane solvents to the Kramers model.[21] This view that the intrinsic barrier for stilbene isomerization in the alkane homologous solvent series is solvent dependent has been challenged by Saltiel and co-workers as they find, on the

S1089-5639(98)00197-2 CCC: $15.00
Published on Web 02/12/1998

basis of the medium-enhanced barrier model, that the intrinsic potential energy barrier is constant throughout the *n*-alkane solvent series.[18] This suggestion of solvent-independent isomerization barrier is further supported by the Saltiel−Waldeck study of the photoisomerization dynamics of *trans*-4,4′-dimethylstilbene, *trans*-4,4′-dimethoxystilbene, and *trans*-4,4′-di(*tert*-butyl)-stilbene where they find that the intrinsic energy barriers for the photoisomerization of these various substituted stilbenes are constant in the *n*-alkane solvent series.[20]

Since the reaction pathway for the ring closure for the above-mentioned ylide to form *cis*-diphenyloxirane involves the diffusional motion of two phenyl groups through solution, a process similar to the isomerization of *trans*-stilbene, we have undertaken an investigation of the rate of ring closure for the *trans*-ylide as a function of temperature in a series of alkane solvents. Herein we present the solvent dependence of the rate constants for the ring closure of the *trans*-ylide and the varying success we have had in fitting our data to the Kramers model. In the various fitting procedures employed in this study, we assume that the intrinsic barrier for isomerization in the *n*-alkane solvent series is independent of solvent.

Experimental Details

Solvent and Reagents. All alkanes (Aldrich, highest purity available) used in this study were purified by passage through silver nitrate impregnated alumina. Other methods of purification such as reflux over sulfuric acid followed by distillation from lithium aluminum hydride lead to irreproducible results. *trans*-Diphenyloxirane from Aldrich (TDPO) was recrystallized from hexanes.

Laser Flash Photolysis. The laser flash photolysis apparatus is similar to many reported in the literature and will therefore only be described briefly.[22] Samples are excited by the fourth harmonic of a Nd:YAG laser (Quanta-Ray DCR-2), 0.5 mJ/pulse, 10 ns, and probed by a pulsed a high-pressure mercury lamp. Probe light wavelength is selected by monochromator (Instruments S.A. Inc., model H10) and detected as a function of time by a photomultiplier (Electron Tubes, Inc., model 9816, four dynodes wired). The output current of the photomultiplier is dropped over 50 ohms to ground, and the resulting voltage is measured by a digital oscilloscope (Tektronix, model TDS350) and stored and processed on a Power Macintosh 7100/80.

For these studies, all kinetic traces were modeled as first-order decays, and fits to the data were minimized with the Levenberg−Marquardt algorithm.

Samples were prepared so as to exhibit optical densities of 0.3−0.6 at 266 nm and were bubbled with argon for 10 min prior to experiment to remove oxygen. In agreement with the literature, atmospheric oxygen has no effect on the lifetimes or quenching rates that are measured.[23] The *trans*-ylide produced upon photolysis at TDPO was probed at 470 nm. Typically, the average of five laser pulses yielded acceptable signal to noise. Samples were not stirred during the experiment. Sample temperature was controlled by flowing thermostated water through an aluminum block that surrounds the sample cuvette.

Results

Figure 1 shows the decay of the *trans*-ylide at 23.5 °C in heptane, monitored at 470 nm, following the 266 nm irradiation of TDPO and the corresponding fit of the model assuming first-order decay. Table 1 lists the first-order rate constants for the decay of the *trans*-ylide as a function of solvent and temperature. Two standard deviations in the uncertainty to the first-order fit

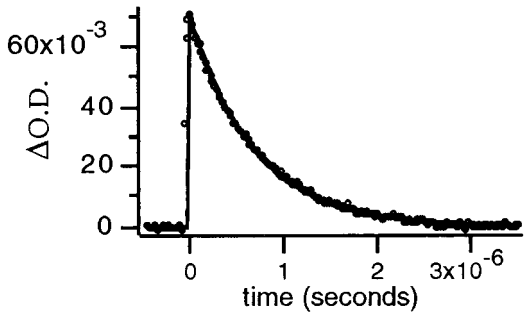

Figure 1. Decay of the *trans*-ylide at 23.5 °C in heptane monitored at 470 nm following the 266 nm irradiation of *trans*-2,3-diphenyloxirane.

TABLE 1: First-Order Rate Constants for the Decay of the *trans*-Ylide as a Function of Temperature and *n*-Alkane Solvent[a]

temp, °C	C5	C6	C7	C8	C9	C10	C12	C14	C16
−5.9	3.21	3.23	3.00	2.78	2.56	2.20	2.25		
−3.7	3.45	3.57	3.47	3.21	2.97	2.66	2.39		
0.8	4.66	4.83	4.15	3.66	3.65	3.51	3.13		
4.7	6.17	5.50	5.19	4.55	4.54	4.29	4.06		
10.0	7.91	7.36	6.50	6.16	6.35	5.73	5.40	5.19	
14.4	9.99	9.38	8.60	7.87	6.96	7.04	7.14	6.56	
18.9	12.7	11.4	11.7	10.5	9.24	9.66	9.04	8.71	
23.5	15.4	14.4	14.0	13.8	12.3	11.9	11.1	10.8	10.7
27.8	19.6	18.7	17.5	16.9	16.2	15.3	14.1	13.7	12.6
32.5		23.8	21.4	21.4	20.3	19.6	18.6	17.4	17.4
37.0		29.6	27.5	25.8	25.0	24.3	23.7	22.8	21.8
41.2		38.8	34.3	32.1	30.1	31.0	28.7	27.1	27.5
45.9		45.7	45.1	39.4	37.4	38.0	34.7	35.6	33.4
50.0									41.8
54.8									50.5

[a] Units are 1×10^5 s^{-1}.

TABLE 2: Fitting Parameters from the Arrhenius Analysis of Kinetic Data in Table 1

	E_a (kcal/mol)	ln A	A (s^{-1})
C5	8.63 ± 0.13	28.92 ± 0.24	3.64×10^{12}
C6	8.71 ± 0.15	29.03 ± 0.26	4.05×10^{12}
C7	8.76 ± 0.15	29.05 ± 0.27	4.11×10^{12}
C8	8.86 ± 0.15	29.15 ± 0.26	4.58×10^{12}
C9	8.82 ± 0.15	29.03 ± 0.27	4.04×10^{12}
C10	9.21 ± 0.09	29.66 ± 0.16	7.59×10^{12}
C12	9.16 ± 0.09	29.51 ± 0.16	6.56×10^{12}
C14	9.57 ± 0.11	30.15 ± 0.20	1.24×10^{13}
C16	9.83 ± 0.19	30.54 ± 0.31	1.84×10^{13}

to the data is less than ±1% of the magnitude of the rate constant. Uncertainty in the temperature for each point is ±0.2 °C, which translates into an uncertainty in rate constant at a given temperature of approximately 1%. Examining Table 1, one observes that the rate constant for the closure of the ylide increases with temperature for a given solvent and decreases with increasing solvent chain length at constant temperature.

An Arrhenius analysis of the experimental data presented in Table 1 was undertaken, and the resulting A factor and E_a for each solvent are given in Table 2. An example of an Arrhenius plot is shown in Figure 2.

Discussion

Kramers Model. In 1940, Kramers presented a model, based upon the Langevin equation, for the escape of a Brownian particle over a one-dimensional barrier. The rate expression for this process takes the form[9]

$$k_{obs} = (\omega/2\pi)(\beta/2\omega')\{[1 + (2\omega'/\beta)^2]^{1/2} - 1\} \exp(-E_0/RT) \quad (1)$$

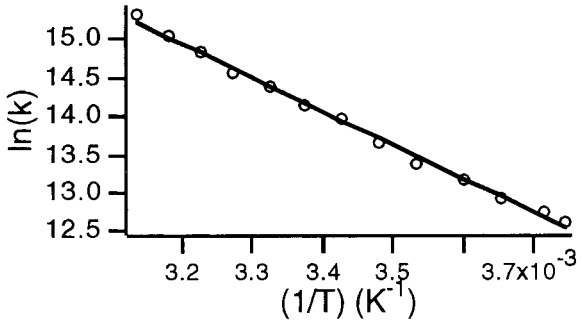

Figure 2. Arrhenius analysis of the kinetics for the decay of the *trans*-ylide in heptane over the temperature range −5.9 °C to 45.9 °C, resulting in $A = 4.11 \times 10^{12}$ s^{-1} and $E_a = 8.76$ kcal/mol.

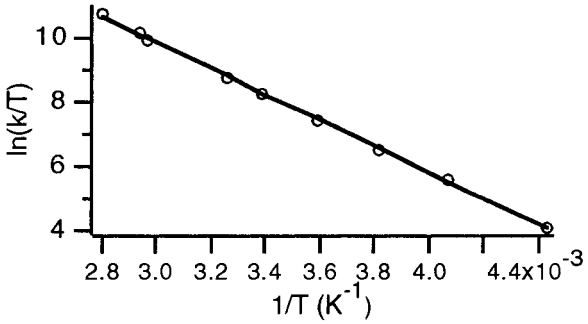

Figure 3. Isomicroviscosity analysis of the kinetic data for the decay of the *trans*-ylide at 0.3 cP.

where ω is the frequency of the parabolic reactant well and ω' is the frequency associated with the curvature of the potential energy surface at the transition state. The energy of the reaction barrier is E_0. The interaction of the particle with the medium is described by the reduced friction coefficient, β, which is equal to the ratio of the friction coefficient ξ_r divided by the particle's moment of inertia, I.

One of the great difficulties in the application of the Kramers model to reacting systems is the determination of the friction coefficient ξ_r for the system. In some of the earlier studies of the dynamics of the isomerization of *trans*-stilbene and related polyenes, it was assumed, employing the Stokes−Einstein hydrodynamic equation, that the friction coefficient could be related to the solvents shear viscosity η_s, $\xi_r \sim \eta_s$.[9,12,24] However, this assumption was found to lead to a poor fit of the Kramers model to the experimental data, leading to the conclusion that macroscopic shear viscosity is an inadequate description for the solute's interaction with the solvent at the molecular level.[13] Substantially improved fits for the Kramers model were found when the friction coefficient ξ_r was related to the friction coefficients derived from the measurement of the solvent dependence of the molecule's rotational reorientation times.[15,17]

Saltiel and co-workers have recently developed a microviscosity model for the measure of the solvent friction for the isomerization of *trans*-stilbene in alkane solvents which is derived from translational diffusion coefficients of toluene in the *n*-alkane solvents.[19] Although the translational diffusion coefficient is proportional to the solvent's viscosity, the proportionality constant will differ from solvent to solvent. Thus, the microviscosity, η_μ, can be related to the shear viscosity, η_s, through a proportionality constant f which is obtained from the ratio of diffusion coefficient from the Stokes−Einstein equation assuming stick boundary conditions, D_{SE}, and the experimental diffusion coefficient, D_{exp}, $f = D_{SE}/D_{exp}$.

$$\eta_\mu = f\eta_s \tag{2}$$

Employing microviscosities, they found that the Kramers model gives an excellent fit to the kinetics for the isomerization of *trans*-stilbene in a wide range of *n*-alkane solvents.

The experimental rate constants can be modeled by the Kramers equation by assuming that the rate expression has the form[9]

$$k_{obs} = F(\eta) \exp(-E_0/RT) \tag{3}$$

where $F(\eta)$ is the dynamical factor, often termed the "reduced isomerization rate". Thus, for a Kramers analysis, it is necessary to isolate the reduced isomerization rate by determining E_0. A common method for obtaining the intrinsic energy of activation is to examine the rate constant for a given process in a homologous solvent series at various temperatures where the temperatures are chosen so that the solvent friction remains constant throughout the temperature range.[9] If the solvent friction is assumed to be proportional to the solvent viscosity or microviscosity, then an isoviscosity plot will yield the intrinsic energy of activation. A fundamental assumption in this analysis is that E_0 does not change in the homologous solvent series so that the derived E_0 should be independent of the viscosity chosen for the isoviscosity plot.

TABLE 3: Energy of Activation, E_0, Derived from Isoviscosity (η) and Isomicroviscosities (η_μ)

η (cP)	E_0 (kcal/mol)	η_μ (cP)	E_0 (kcal/mol)
0.1	10.32 ± 0.53	0.1	9.29 ± 0.30
0.2	9.30 ± 0.27	0.2	8.67 ± 0.13
0.3	9.00 ± 0.21	0.3	8.47 ± 0.11
0.5	8.72 ± 0.14	0.5	8.42 ± 0.06
1.0	8.59 ± 0.09	1.0	8.29 ± 0.04
2.0	8.45 ± 0.04	2.0	8.20 ± 0.05
4.0	8.39 ± 0.05	4.0	8.17 ± 0.06

In our attempt to model the rate of ring closure for the ylide within Kramers formulation, we assume that solvent friction can be related to either the shear viscosity or the microviscosity derived from the translation diffusion of toluene in the *n*-alkane solvents, following the method of analysis developed by Saltiel for *trans*-stilbene isomerization.[19] The temperature dependence of the microviscosity η_μ was derived from the temperature dependence of the shear viscosity η_s and from the assumption that the f factor ($f = D_{SE}/D_{exp}$) is temperature independent. The temperature dependence of the shear viscosity is calculated from the Andrade equation,[9]

$$1/\eta = A_\eta \exp(-E_\eta/RT) \tag{4}$$

The results of both the isoviscosity and isomicroviscosity are given in Table 3, and a plot of the isomicroviscosity for 0.3 cP is shown in Figure 3. The kinetics for the isoviscosity plots were obtained from the extrapolation of the temperature dependence of the kinetic data assuming an Arrhenius type of behavior. Surprisingly, for the isoviscosity analysis the derived energy of activation decreases from 10.3 kcal/mol for 0.1 cP to 8.4 kcal/mol for 4.0 cP. Similarly, the isomicroviscosity plots yield an energy of activation of 9.2 kcal/mol, which decreases to 8.2 kcal/mol for a change in microviscosity of 0.1 to 4.0.

For a Kramers analysis of a kinetic process that employs a homologous solvent series, such as the *n*-alkanes, as a means of systematically varying the solvent friction, one assumes that the energy of the reaction barrier does not change with solvent. Clearly this is not observed in the present study of ylide ring closure in *n*-alkane solvents. Therefore, either the viscosity or microviscosity is not a good measure of the solvent friction felt

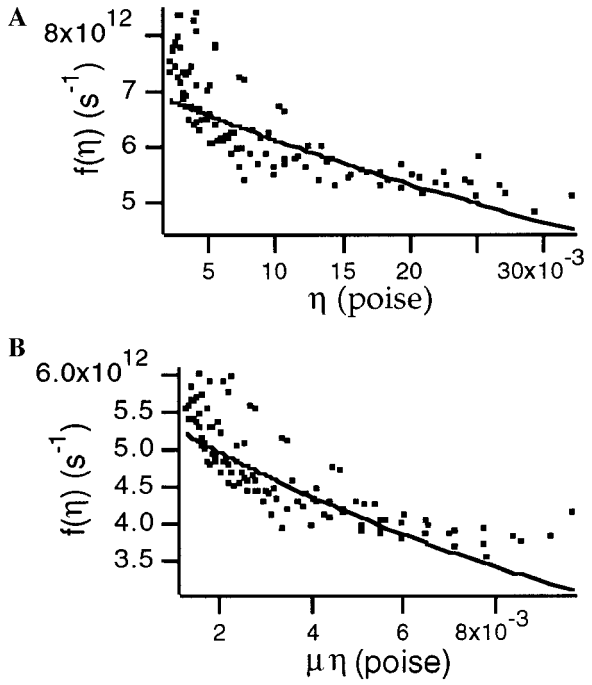

Figure 4. (A) Kramers analysis of kinetic data given in Table 1 employing solvent shear viscosity, η. Resulting parameters $E_0 = 9.06$ kcal/mol, $A = 6.99 \times 10^{12}$ s^{-1}, and $B = 14.2$ P^{-1}. (B) Kramers analysis of kinetic data given in Table 1 employing microviscosity, η_μ. Resulting parameters $E_0 = 8.88$ kcal/mol, $A = 5.67 \times 10^{12}$ s^{-1}, and $B = 65.4$ P^{-1}.

by the ring closure process or the Kramers model is not applicable to the observed kinetic process. It is also possible that the energy of activation is dependent upon the chain length of the alkane solvent.[21]

Instead of deducing the energy of activation, E_0, from isoviscosity plots in order that the reduced isomerization rate may be obtained, it is feasible to fit the Kramers model given in eq 1 by not only varying the parameters in the preexponential term but also allowing E_0 to vary as well. It is convenient to reformulate eq 1 so that the observed rate is expressed as[9]

$$k_{obs} = A[(1 + (\eta B)^2)^{1/2} - \eta B] \exp(-E_0/RT) \qquad (5)$$

where $A = \omega_0/2\pi$ and $\eta B = (2\omega'\tau_v)^{-1}$. The term η can be either the shear viscosity or the microviscosity for the present analysis, and the velocity relaxation τ_v is given by $\tau_v = \mu/\xi$ where ξ is the friction coefficient and μ is the reduced mass.

Since a single activation barrier is not obtained in the isoviscosity analysis, we have attempted to fit our data to eq 5 by varying A, B, and E_0 to minimize the square of the residuals. The fit is shown in Figure 4 where the reduced isomerization rate $F(\eta)$ is obtained from experimental data and the parameter E_0, $F(\eta) = k_{obs} \exp(E_0/RT)$. Clearly the model cannot account for the curvature in the correlation of $F(\eta)$ with η. Also, the range in the scatter of the data at a given viscosity or microviscosity is substantially greater that the error in the experimental data. This scatter presumably results from the assumption in this last fitting procedure that E_0 is independent of the solvent.

Grote−Hynes Model. The apparent breakdown of the Kramers model for describing the frictional dependence of the rate for ring closure in *trans*-ylide may possibly be traced to the assumption that either viscosity or microviscosity is a measure of the solvent friction felt by the isomerizing molecule in the transition state. Grote and Hynes have suggested that forces acting on the isomerization coordinate should relax on the time scale associated with the passage of the reacting molecule through the transition state so that the friction on the reacting system becomes frequency dependent; thus, the friction is a sensitive function of the nature of the intrinsic reaction barrier.[25] This would suggest that even though the microviscosity derived from diffusion coefficients of toluene appears to be a good measure of the friction encountered in the isomerization of *trans*-stilbene, a process whose intrinsic barrier is 2.8 kcal/mol in the *n*-alkane solvents, the same microviscosities are not transferable as a measure of friction in the ring closure of the *trans*-ylide, a process whose intrinsic barrier is of the order of 8−9 kcal/mol.[18]

The theoretical model employing a frequency-dependent friction developed by Grote and Hynes has been applied to several reacting systems. In 1982, Bagchi and Oxtoby used a hydrodynamic model for the frequency-dependent friction to fit the experimental values for the rate of photoisomerization of *trans*-diphenylbutadiene and DODCI as a function of temperature in a variety of solvents.[26] Velsko, Waldeck, and Fleming have examined the breakdown of Kramers theory for the photochemical isomerization of DODCI within the framework of a frequency-dependent friction.[27] Finally, Hochstrasser and co-workers have applied the Grote−Hynes model to their experimental studies of the rate of photoisomerization of *trans*-stilbene.[28]

Since the application of the Kramers model, employing a hydrodynamic model for the friction, fails to account for the observed solvent dependence of the rate for ring closure of the *trans*-ylide, we have analyzed our experimental data within Grote−Hynes theory[25] employing the hydrodynamic model developed by Bagchi and Oxtoby for the frequency-dependent friction.[26] The rate constant for reaction, k, given by Grote−Hynes theory is

$$k = k^{TST}(\lambda_r/\omega_b) \qquad (6)$$

where k^{TST} is the rate constant for the reaction predicted by transition-state theory,

$$k^{TST} = (\omega_R/2\pi) \exp(-E_0/RT) \qquad (7)$$

and ω_R is the frequency in the reactant well, ω_b is the reaction barrier frequency, and λ_r is reactive frequency given by

$$\lambda_r = \omega_b{}^2/(\lambda_r + \zeta(\lambda_r)/\mu) \qquad (8)$$

The term $\zeta(\lambda_r)$ is the Laplace transform of the time-dependent friction, and μ is the moment of inertia of the twisting group.

For the isomerization of the *trans*-ylide, the phenyl groups will experience a friction arising from the sum of two sources: a rotational friction, ζ_r, and a translation friction, $(R + l)^2\zeta_{tr}$, where R is the hydrodynamic radius of the phenyl group and l is the distance between the oxygen atom and the carbon atom to which the phenyl group is attached.[26]

An expression for the frequency dependence of the translational friction, $\zeta_{tr}(p)$, was derived by Zwanzig and Bixon[29] and modified by Metiu, Oxtoby and Freed.[30] Similarly, an expression for the frequency dependence of the rotational friction, $\zeta_r(p)$, was derived by Berne and Montgomery.[31] The expressions for $\zeta_{tr}(p)$ and $\zeta_r(p)$ depend on the frequency-dependent shear viscosity, $\eta_s(p)$, the frequency-dependent bulk viscosity, $\eta_v(p)$, the solvent density, ρ_0, the velocity of sound, c, the slip parameter, β, and hydrodynamic radius, R. The frequency dependence of the shear viscosity, $\eta_s(p)$, and the bulk viscosity,

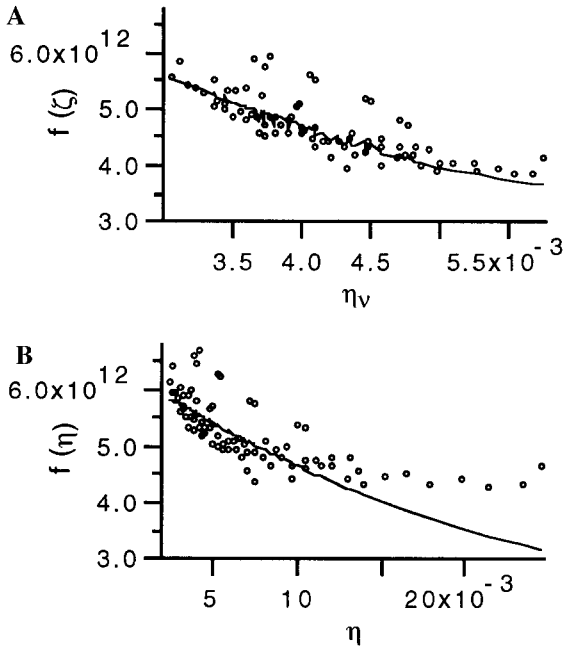

Figure 5. (A) Grote−Hynes analysis of the kinetic data given in Table 1 where the data for pentane, tetradecane, and hexadecane are removed. The fitting parameters are $\omega_R = 6.6 \times 10^{13}$ s^{-1}, $\omega_b = 1.2 \times 10^{13}$ s^{-1}, and $E_0 = 8.9$ kcal/mol. $f(\zeta)$ and η_v are defined in the text. (B) Kramers analysis of kinetic data given in Table 1 employing solvent shear viscosity, η, where the data for pentane, tetradecane, and hexadecane are removed. Resulting parameters $E_0 = 9.06$ kcal/mol, $A = 6.99 \times 10^{12}$ s^{-1}, and $B = 14.2$ P^{-1}.

$\eta_v(p)$, is assumed to be given by the Maxwell forms

$$\eta_s(p) = \eta_s^0/(1 + p\tau_s)$$

$$\eta_v(p) = \eta_v^0/(1 + p\tau_v) \quad (9)$$

where η_s^0 is the zero-frequency shear viscosity and η_v^0 is the zero-frequency bulk viscosity. The times τ_s and τ_v are the viscoelastic relaxation times. For the detail expressions for $\zeta_{tr}(p)$, $\zeta_r(p)$, τ_s, and τ_v, see the work of Bagchi and Oxtoby.[26]

The values of the solvent parameters—shear viscosity, bulk viscosity, speed of sound, density, and their associated temperature dependencies—can be found in refs 32−36. Values for the solvents pentane, tetradecane, and hexadecane could not be found, and thus the data for these solvents were removed from the gobal analysis. The remaining quantities R, μ, and l were obtained molecular mechanic calculations producing the values $R = 2.6$ Å, $l = 1.8$ Å, and $\mu = 9.7 \times 10^{-8}$ g cm^2.

Employing a Simplex nonlinear least-squares routine to vary ω_R, ω_b, and E_0, the three fitting parameters,[37] we found that $\omega_R = 6.6 \times 10^{13}$ s^{-1}, $\omega_b = 1.2 \times 10^{13}$ s^{-1}, and $E_0 = 8.9$ kcal/mol. The fit of the reduced data set to the Grote−Hynes theory employing the Bagchi−Oxtoby frequency-dependent hydrodynamic model with slip boundary conditions[26] is shown in Figure 5A where the reduced rate constant defined by

$$f(\zeta) = (\omega_R/2\pi)(\lambda_r/\omega_b) \quad (10)$$

is correlated with frequency-dependent shear viscosity, $\eta_v(p)$. For comparison, the fits of the Kramers model to the same reduced data set are shown in Figure 5B. Clearly, the Grote−Hynes model gives a significantly better fit to the experimental data than the Kramers model, particularly for the data at higher viscosities.

Even though the Grote−Hynes model gives a superior fit to the experimental data, there is still substantial deviation between the experiment and the model where the deviation is larger than the experimental error in the data. One source of error in the modeling is the assumption of the Maxwell form for the frequency dependence of the bulk and shear viscosities since there are no measurements of the viscoelastic response for the solvents at the reactant frequencies.

Another possibility for the breakdown of the Kramers theory or Grote−Hynes theory is that the reaction coordinate for the ring closure of the *trans*-ylide is inherently multidimensional so that modeling the reaction as a process corresponding to the escape of a Brownian particle over a one-dimensional barrier becomes inappropriate. Models for the dynamics of two-dimensional diffusional barrier crossings have recently been presented.[38] One could imagine that in the absence of solvent the intrinsic reaction path connecting the *trans*-ylide to CDPO has the phenyl rings rotating with the methylene groups such that the charge/radical character that might otherwise be localized on the methylene carbons may be delocalized into the phenyl π-orbitals. When placed in a solvent, this intrinsic reaction path may require the phenyl rings to move a maximum number of solvent molecules out of the path, and so, as a function of solvent, the phenyl rings may rotate so that they slice more through the solvent, even through this lessens the conjugation between the methylene groups and the phenyl rings at the transition-state geometry. Thus, the intrinsic energy of activation becomes solvent dependent, reflecting different reaction paths through the transition state.

Conclusions

The original aim of this study was to ascertain whether the Kramers model would be effective in describing the reaction dynamics for ring closure of the *trans*-ylide to form CDPO. We found that the data could not be modeled within the Kramers framework and that it was necessary to employ Grote−Hynes theory to give a significantly better fit to the experimental data. However, the fit is still less than ideal, perhaps reflecting that the reaction coordinate cannot be model as a one-dimensional process. In the future we plan to examined ring closure of ylides whose phenyl groups are modified so as to prevent the rotation of phenyl groups with respect to the methylene centers during the ring closure process, thus reducing the dimensionality of the reaction coordinate.

Acknowledgment. This work is supported by a grant from the National Science Foundation, CHE 9408354.

References and Notes

(1) Houk, K. N.; Li, Y.; Evanseck, J. D. *Angew. Chem., Int. Ed. Engl.* **1992**, *31*, 682−708.
(2) Jorgensen, W. L.; Blake, J. F.; Lim, D.; Severance, D. L. *J. Chem. Soc., Faraday Trans.* **1994**, *90*, 1727−1732.
(3) Lim, D.; Jorgensen, W. J. *J. Phys. Chem.* **1996**, *100*, 17490−17500.
(4) Doubleday, C.; Bolton, K.; Peslherbe, G. H.; Hase, W. L. *J. Am. Chem. Soc.* **1996**, *118*, 9922−9931.
(5) Carpenter, B. K. *J. Am. Chem. Soc.* **1995**, *117*, 6336−6344.
(6) Carpenter, B. K. *J. Am. Chem. Soc.* **1996**, *118*, 10329−10330.
(7) Horn, B. A.; Herek, J. L.; Zewail, A. H. *J. Am. Chem. Soc.* **1996**, *118*, 8755−8756.
(8) Lipson, M.; Peters, K. S. *J. Org. Chem.*, submitted for publication.
(9) Waldeck, D. H. *Chem. Rev.* **1991**, *91*, 415−436.
(10) Kramers, H. A. *Physica* **1940**, *7*, 284.
(11) Courtney, S. H.; Fleming, G. R. *J. Chem. Phys.* **1985**, *83*, 215−222.
(12) Velsko, S. P.; Fleming, G. R. *J. Chem. Phys.* **1982**, *76*, 3553−3562.

(13) Velsko, S. P.; Waldeck, D. H.; Fleming, G. R. *J. Chem. Phys.* **1983**, *78*, 249−258.
(14) Bowman, R. M.; Eisenthal, K. B. *Chem. Phys. Lett.* **1989**, *155*, 99−101.
(15) Lee, M.; Bain, A. J.; McCarthy, P. J.; Han, C. H.; Haseltine, J. N.; Smith III, A. B.; Hochstrasser, R. M. *J. Chem. Phys.* **1986**, *85*, 4341−4347.
(16) Lee, M.; Haseltine, J. N.; Smith III, A. B.; Hoschstrasser, R. M. *J. Am. Chem. Soc.* **1989**, *111*, 5044−5051.
(17) Kim, S. K.; Fleming, G. R. *J. Phys. Chem.* **1988**, *92*, 2168−2172.
(18) Saltiel, J.; Sun, Y.-P. *J. Phys. Chem.* **1989**, *93*, 6246−6250.
(19) Sun, Y.-P.; Saltiel, J. *J. Phys. Chem.* **1989**, *93*, 8310−8316.
(20) Sun, Y.-P.; Saltiel, J.; Park, N. S.; Hoburg, E. A.; Waldeck, D. H. *J. Phys. Chem.* **1991**, *95*, 10336−10344.
(21) Schroeder, J.; Troe, J.; Vohringer, P. *Z. Phys. Chem.* **1995**, *188*, 287−306.
(22) Scaiano, J. C. In *CRC Handbook of Organic Photochemistry*; Scaiano, J. C., Ed.; CRC Press: Boca Raton, 1989.
(23) Kumar, C. V.; Chattopadhyay, S. K.; Das, P. K. *J. Phys. Chem.* **1984**, *88*, 5639−5643.
(24) Lee, M.; Bain, J.; McCarthy, P. J.; Han, C. H.; Haseltine, J. N.; Smith III, A. B.; Hochstrasser, J. M. *J. Chem. Phys.* **1986**, *85*, 4341−4347.
(25) Grote, R. F.; Hynes, J. T. *J. Chem. Phys.* **1980**, *73*, 2715.
(26) Bagchi, B.; Oxtoby, D. W. *J. Chem. Phys.* **1983**, *78*, 2735−2741.
(27) Velsko, S. P.; Waldeck, D. H.; Fleming, G. R. *J. Chem. Phys.* **1983**, *78*, 249−258.
(28) Rothenberger, G.; Negus, D. K.; Hochstrasser, R. M. *J. Chem. Phys.* **1983**, *79*, 5360−5367.
(29) Zwanzig, R.; Bixon, M. *Phys. Rev. A* **1970**, *2*, 2005−2012.
(30) Metiu, H.; Oxtoby, D. W.; Freed, K. F. *Phys. Rev. A* **1977**, *15*, 361−371.
(31) Montgomery, Jr., J. A.; Berne, B. J. *J. Chem. Phys.* **1977**, *66*, 2161−2771.
(32) Riddick, J. A.; Bunger, W. B.; Sakano, T. K. *Organic Solvents: Physical Properties and Methods of Purification*, 4th ed.; John Wiley & Sons: New York, 1986; Vol. II.
(33) Nozdrev, V. F. *The Use of Ultrasonics in Molecular Physics;* The Macmillan Company: New York, 1965.
(34) Piercy, J. E.; Rao, M. G. S. *J. Chem. Phys.* **1967**, *46*, 3951−3959.
(35) Patterson, G. D.; Lindsey, C. P. *J. Appl. Phys.* **1978**, *49*, 5039−5041.
(36) Boelhouwer, J. W. M. *Physica* **1967**, *34*, 484−492.
(37) Press, W. H. *Numerical Recipes: The Art of Scientific Computing;* Cambridge University Press: New York, 1986.
(38) Agmon, N.; Kosloff, R. *J. Phys. Chem.* **1987**, *91*, 1988−1996.